

Chemical Twinning of the Rock Salt Structure: CaTi_2O_4 and $\text{Ca}_2\text{Ti}_2\text{O}_5$, the First Two Members of the New Series $\text{Ca}_n\text{Ti}_2\text{O}_{n+3}$

F. Goutenoire, V. Caignaert, M. Hervieu, C. Michel, and B. Raveau

Laboratoire CRISMAT, CNRS URA 1318, ISMRA, Université de Caen, Boulevard du Maréchal Juin, 14050 Caen Cedex, France

Received March 10, 1994; accepted May 25, 1994

Two new calcium thallates, CaTi_2O_4 and $\text{Ca}_2\text{Ti}_2\text{O}_5$, have been isolated that crystallize in the $Cmcm$ space group with $a \approx 3.3255(1) \text{ \AA}$, $b = 11.022(1) \text{ \AA}$, and $c = 10.479(1) \text{ \AA}$ for the first and $a = 3.3431(1) \text{ \AA}$, $b = 11.159(1) \text{ \AA}$, and $c = 13.499(1) \text{ \AA}$ for the second. The *ab initio* determination of their structure from powder X-ray data shows that they are closely related and that they represent the first two members of a series with the generic formula $\text{Ca}_n\text{Ti}_2\text{O}_{n+3}$. In fact, the first member, CaTi_2O_4 , is isotypic to CaTi_2O_4 and can be described as a chemical twin of $[\text{Ti}_2\text{O}_4]_\infty$ rock salt layers, whereas the second member, $\text{Ca}_2\text{Ti}_2\text{O}_5$, is derived from the first by increasing the thickness of the rock salt layers, i.e., by replacing double ribbons of edge-sharing octahedra by triple ribbons. In both structures, the chemical twinning is induced by the ability of calcium to adopt the trigonal prismatic coordination in prismatic tunnels; the direction of rock salt layer is invariable, i.e., parallel to the (113) plane of the cubic rock salt structure. © 1995 Academic Press, Inc.

INTRODUCTION

The discovery of superconductivity at high temperatures in thallium cuprates (1) has raised the issue of the role played by noncopper rock-salt-type layers in the properties of these materials. In such layers, trivalent thallium is associated with alkaline earth cations according to the formulations $[(\text{TlO})_2(\text{AO})]_\infty$ or $[(\text{TlO})(\text{AO})]_\infty$ with $A = \text{Ba}, \text{Sr}$. It has been proposed that the thallium oxygen layers play the role of hole reservoirs for the copper oxygen layers (2); this hypothesis is supported by electronic structure calculations (3-6). Thus, it is of great interest to understand the chemistry and physics of alkaline earth thallates. One barium thallate, $\text{Ba}_2\text{Ti}_2\text{O}_5$ (7) with the Brownmillerite structure, and two strontium thallates, $\text{Sr}_4\text{Ti}_2\text{O}_7$ (8) and SrTi_2O_4 (9), have been synthesized to date. Curiously, no calcium thallate has been isolated to our knowledge. We report here on two new phases, CaTi_2O_4 and $\text{Ca}_2\text{Ti}_2\text{O}_5$, whose structures are closely related to that of CaTi_2O_4 and can be described as chemical twins of the rock salt structure.

EXPERIMENTAL

The oxides CaTi_2O_4 and $\text{Ca}_2\text{Ti}_2\text{O}_5$ were prepared from mixtures of oxides Ti_2O_3 and CaO , in stoichiometric molar ratios, mixed in an agate mortar. The mixtures, placed in an alumina crucible, were progressively heated in an evacuated silica tube to 750°C . They were kept at this temperature for 12 hr for CaTi_2O_4 and for 48 hr for $\text{Ca}_2\text{Ti}_2\text{O}_5$. The microcrystalline powders were brown for CaTi_2O_4 and orange-brown for $\text{Ca}_2\text{Ti}_2\text{O}_5$.

The powder X-ray diffraction data were collected by step scanning over an angular range $15^\circ \leq 2\theta \leq 120^\circ$ for CaTi_2O_4 and $12^\circ \leq 2\theta \leq 120^\circ$ for $\text{Ca}_2\text{Ti}_2\text{O}_5$ with an increment of $0.02^\circ (2\theta)$, using a Philips PW 3710 diffractometer with $\text{CuK}\alpha$ radiation. The X-ray patterns were used to refine the structure with the profile computer program FULLPROF (10).

The electron diffraction (ED) study of the microcrystals of both phases was performed with a JEOL 200CX electron microscope fitted with an eucentric goniometer ($\pm 60^\circ$).

RESULTS AND DISCUSSION

For the experimental conditions described above $\text{Ca}_2\text{Ti}_2\text{O}_5$ could be synthesized as a single phase, whereas CaTi_2O_4 was obtained as an almost single phase, mixed with an unknown phase as an impurity.

In the first step the cell parameters have been found by an autoindexing program TREOR4 (11).

The ED investigation of these two phases evidenced one orthorhombic cell with two similar parameters for the two compounds ($a \sim 3.3 \text{ \AA}$, $b \sim 11 \text{ \AA}$) and a third parameter c of 10.5 and 13.5 \AA for CaTi_2O_4 and $\text{Ca}_2\text{Ti}_2\text{O}_5$, respectively. The systematic absences hkl , $h + k = 2n + 1$, and $h0l$, $l = 2n$, lead to the space group $Cmcm$ for both structures as shown from the [100] and [001] ED patterns in Fig. 1.

Both structures were solved *ab initio* with the same procedure. The integrated intensities were extracted from the data in the range $12^\circ < 2\theta < 70^\circ$ by a full pattern

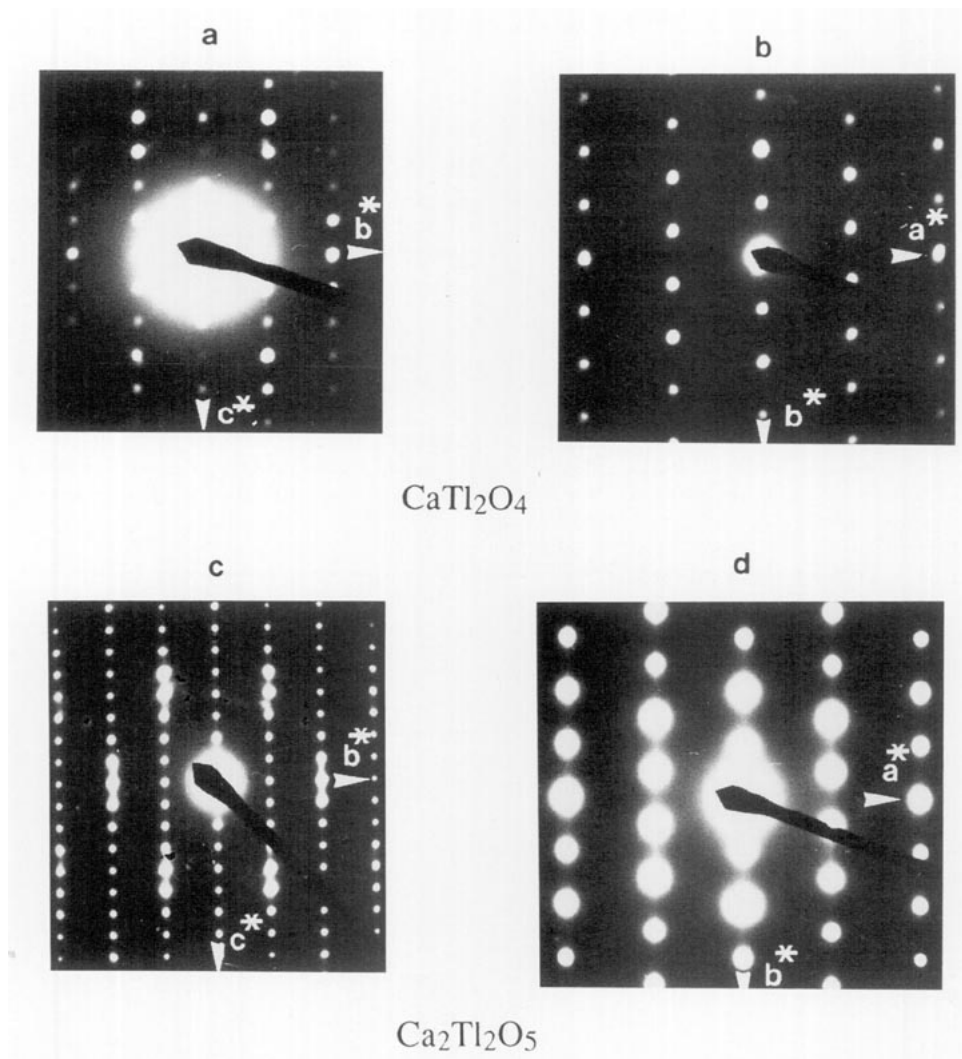


FIG. 1. (a) [100] and (b) [001] ED patterns of CaTi_2O_4 ; (c) [100] and (d) [001] ED patterns of $\text{Ca}_2\text{Ti}_2\text{O}_5$.

decomposition method with the FULLPROF (10) program. The structure factors obtained were used to generate Patterson maps. In the case of CaTi_2O_4 , the resolution

TABLE 1
Crystallographic Parameters of CaTi_2O_4

Atom	Site	x	y	z	B (\AA^2)
Tl	8f	0.0	0.3652(1)	0.0725(1)	0.19(3)
Ca	4c	0.0	0.1076(6)	0.25	0.2(2)
O_1	8f	0.0	0.287(1)	0.628(1)	0.5(2) ^a
O_2	4a	0.0	0.0	0.0	0.5(2) ^a
O_3	4c	0.0	0.461(2)	0.25	0.5(2) ^a

Note. Space group: $Cmcm$; $Z = 4$. Cell parameters: $a = 3.3255(1)$ \AA , $b = 11.022(1)$ \AA , and $c = 10.479(1)$ \AA . $\chi^2 = 5.35$, $R_p = 19.3\%$, $R_{wp} = 23.9\%$, $R_i = 8.96\%$.

^a B factors for oxygen are refined together.

of the Patterson function allowed the thallium ions to be easily located from the very strong Tl–Tl peaks. The resolution was more complicated for $\text{Ca}_2\text{Ti}_2\text{O}_5$, due to the presence of a mixed site occupied by calcium and thallium simultaneously, leading to “Tl–Ca” peaks corresponding to different sites. For both compounds, the positions of thallium were obtained and formed the initial model for Rietveld refinements using the FULLPROF (10) program. The calcium and oxygen sites were located after subsequent cycles of refinement and difference Fourier syntheses. The atomic coordinates of all atoms, the occupancy factors of the metallic sites, and the isotropic thermal factors B of the metallic atoms were refined successively. The B factors of the oxygen atoms were fixed at 1 \AA^2 or refined together due to their low scattering power. The reliability factor was lowered to $R_i = 0.079$ for $\text{Ca}_2\text{Ti}_2\text{O}_5$, whereas it could only be lowered to $R_i = 0.089$ for CaTi_2O_4 owing to the presence of the unknown impurity (Fig. 2a).

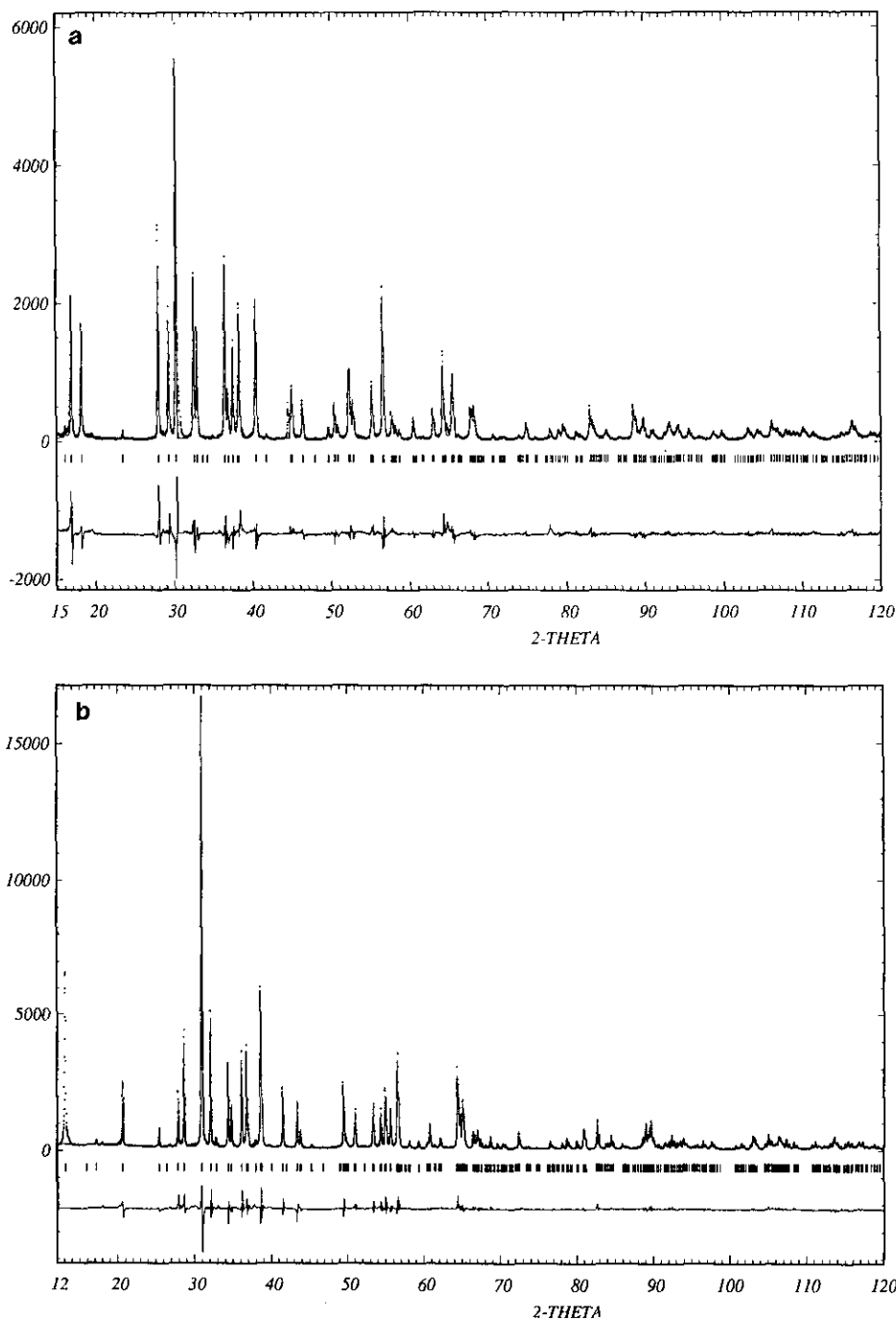


FIG. 2. (a) XRD patterns of CaTi_2O_4 (experimental, calculated, and difference); (b) XRD patterns of $\text{Ca}_2\text{Ti}_2\text{O}_5$ (experimental, calculated, and difference).

The final atomic parameters corresponding to these new compounds are listed in Tables 1 and 2.

From this investigation, it clearly appears that the structure of CaTi_2O_4 (Fig. 3) belongs to the CaTi_2O_4 type (12). It can be described from the association of rutile chains, i.e., chains of edge-sharing TiO_6 octahedra running along

a. Along b, each rutile chain shares the edges of its octahedra with a similar chain located at the same level x , and its opposite edges with a second chain shifted $a/2$. As a result the structure consists of double octahedral chains of edge-sharing octahedra located at the same x level (e.g., light shading in Fig. 3) that share their edges with identical

TABLE 2
Crystallographic Parameters of $\text{Ca}_2\text{Ti}_2\text{O}_5$

Atom	Site	x	y	z	Occupation	B (\AA^2)
Tl ₁	8f	0.0	0.7714(2)	0.3857(1)	0.56(2)	0.44(4)
Ca ₁	8f	0.0	0.7714(2)	0.3857(1)	0.44(2)	0.44(4)
Tl ₂	4b	0.0	0.5	0.5	1	0.45(3)
Ca ₂	4c	0.0	0.0309(5)	0.25	1	0.2(1)
O ₁	8f	0.0	0.147(1)	0.0438(1)	1	1 ^a
O ₂	8f	0.0	0.425(1)	0.1423(9)	1	1 ^a
O ₃	4c	0.0	0.668(1)	0.25	1	1 ^a

Note. Space group: $Cmcm$; $Z = 4$. Cell parameters: $a = 3.3431(1) \text{ \AA}$, $b = 11.159(1) \text{ \AA}$, and $c = 13.499(1) \text{ \AA}$. $\chi^2 = 4.87$, $R_p = 14.6\%$, $R_{wp} = 12.1\%$, $R_1 = 7.92\%$.

^a B factors for oxygen are arbitrarily fixed to 1 \AA^2 .

double chains of edge-sharing octahedra but shifted $a/2$ (e.g., dark shading in Fig. 3). Thus, it results in $[\text{Ti}_2\text{O}_4]_\infty$ layers parallel to (001) (Fig. 3) that share the apices of their octahedra, forming prismatic tunnels where the calcium ions are located with a bicapped trigonal prismatic coordination. This ability of CaTi_2O_4 to form edge-sharing rutile chains and prismatic tunnels is very similar to that observed for SrTi_2O_4 (9); nevertheless, the latter oxide,

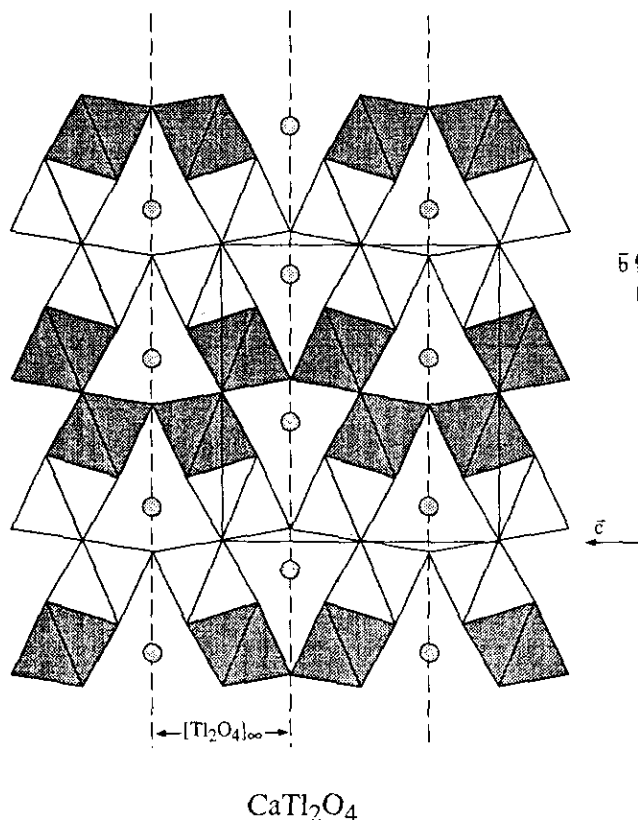


FIG. 3. Projection onto the (100) plane of the structure of CaTi_2O_4 ; darkly and lightly shaded octahedra are shifted $a/2$.

in spite of its close relationships with CaTi_2O_4 , exhibits a different arrangement of the octahedra (Fig. 4) that leads to the CaFe_2O_4 -type structure (13). Thus, it seems that the relative size of the A cations with respect to the B cations in these $AB_2\text{O}_4$ oxides plays an important role in the stabilization of such structures.

Although they cannot be considered as very accurate, the interatomic distances (Table 3) can be considered as significant in agreement with the ionic radii of the elements (14). The Ca–O distances, ranging from 2.32 to 2.39 \AA for the CaO_6 prisms with two additional neighbors at 2.87

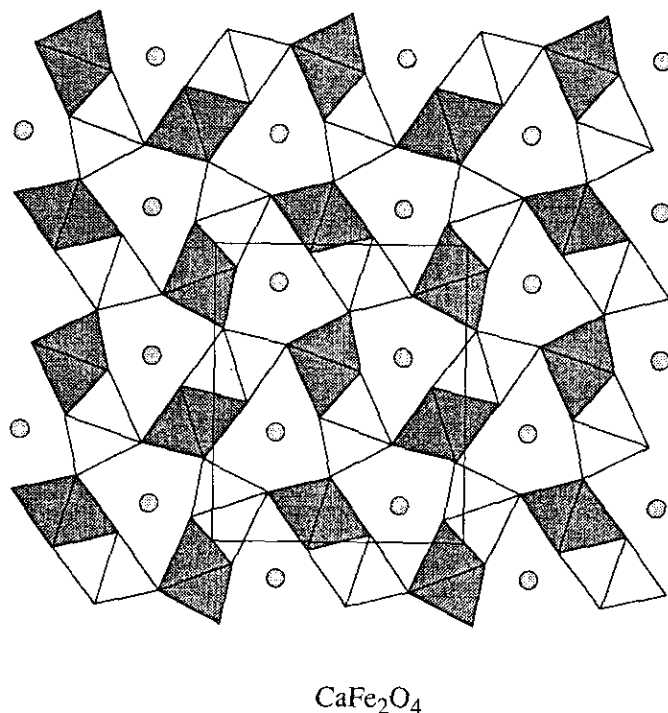


FIG. 4. Projection onto the (001) plane of the structure of CaFe_2O_4 ; darkly and lightly shaded octahedra are shifted $c/2$.

TABLE 3
Interatomic Distances
for CaTi_2O_4 (Å)

Tl-O ₁	2.44(1) (2×)
Tl-O ₁	2.27(1) (1×)
Tl-O ₂	2.356(1) (2×)
Tl-O ₃	2.14(1) (1×)
Ca-O ₁	2.392(1) (4×)
Ca-O ₂	2.876(3) (2×)
Ca-O ₃	2.32(2) (2×)

Å, are similar to those observed for calcium in oxides with this type of coordination. The Tl-O distances ranging from 2.14 to 2.44 Å show that the TlO_6 octahedra are significantly distorted, i.e., slightly more distorted than those in Tl_2O_3 (2.13 to 2.47 Å) (15, 16), but still less distorted than those in the thallium cuprates which systematically exhibit two extra short apical distances (2.0 to 2.06 Å) and four much longer equatorial distances ranging from 2.4 to 2.8 Å (see, for instance, Ref. (1, 17-19)).

The structure of $\text{Ca}_2\text{Tl}_2\text{O}_5$ (Fig. 5) is closely related to that of CaTi_2O_4 (Fig. 3). One indeed recognizes the existence of infinite rutile chains of edge-sharing TlO_6 and CaO_6 octahedra running along *a*, as well as the presence of

identical prismatic tunnels where calcium ions are located with trigonal prismatic coordination. The structure is built up from triple chains of edge-sharing octahedra located at the same level *x* (e.g., light shading in Fig. 5) that share their edges with identical octahedral triple chains but shifted *a*/2 (e.g., dark shading in Fig. 5). In each triple chain, the central chain is occupied by thallium only, whereas the two other chains are half occupied by thallium and half by calcium in a statistical way. Thus, the structure of $\text{Ca}_2\text{Tl}_2\text{O}_5$ consists of $[\text{CaTi}_2\text{O}_5]_\infty$ layers parallel to (001) (Fig. 5) that share the apices of their octahedra in an absolutely identical way as for CaTi_2O_4 (Fig. 3). Consequently, the structure of $\text{Ca}_2\text{Tl}_2\text{O}_5$ can be deduced from that of CaTi_2O_4 by simply replacing the double octahedral ribbons by triple octahedral ribbons, i.e., by just adding chains of edge-sharing octahedra to the $[\text{Tl}_2\text{O}_4]_\infty$ layers.

The interatomic distances (Table 4) are similar to those observed for CaTi_2O_4 . The six shortest Ca-O distances, corresponding to the Ca^{2+} cations of the prismatic tunnels, spread over a larger range (2.27 to 2.51 Å) than those for CaTi_2O_4 ; more significantly, the other oxygen atoms sit much further apart, at distances larger than 3 Å, so that the coordination of Ca^{2+} is purely trigonal prismatic, in contrast to CaTi_2O_4 where it can be described as a bicapped trigonal prism. The distortion of the TlO_6 octahedra (Tl_2) located in the central chains (Fig. 5) is very

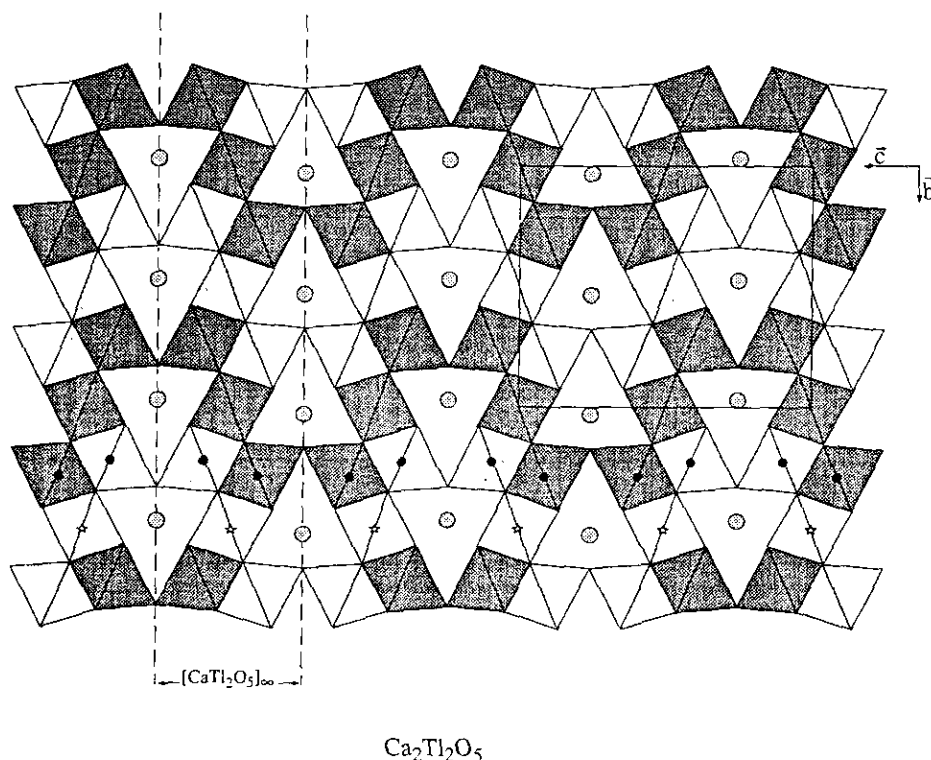


FIG. 5. Projection onto the (100) plane of the structure of $\text{Ca}_2\text{Tl}_2\text{O}_5$; darkly and lightly shaded octahedra are shifted *a*/2. Tl_1 , Ca_1 are depicted by black dots and Tl_2 by white stars.

TABLE 4
Interatomic Distances
for $\text{Ca}_2\text{Ti}_2\text{O}_5$

$(\text{Ti}_1\text{Ca}_1)\text{-O}_1$	2.31(1) (1 \times)
$(\text{Ti}_1\text{Ca}_1)\text{-O}_1$	2.37(1) (2 \times)
$(\text{Ti}_1\text{Ca}_1)\text{-O}_2$	2.42(1) (2 \times)
$(\text{Ti}_1\text{Ca}_1)\text{-O}_3$	2.16(1) (1 \times)
<hr/>	
$\text{Ti}_2\text{-O}_1$	2.42(1) (4 \times)
$\text{Ti}_2\text{-O}_2$	2.09(1) (2 \times)
<hr/>	
$\text{Ca}_2\text{-O}_2$	2.51(1) (4 \times)
$\text{Ca}_2\text{-O}_3$	2.27(1) (2 \times)
$\text{Ca}_2\text{-O}_1$	3.07(1) (2 \times)

similar to that observed for CaTi_2O_4 , with Ti-O distances ranging from 2.09 to 2.42 Å. The $(\text{Ti}, \text{Ca})\text{O}_6$ extreme octahedra of the chains (Ti_1), of the triple octahedral ribbons (Fig. 5), seem to be even less distorted (2.16 to 2.42 Å), perhaps because of the presence of calcium.

The analysis of these two structures shows that they are both closely related to the rock-salt-type structure. The consideration of the $[\text{Ti}_2\text{O}_4]_\infty$ octahedral layers of the CaTi_2O_4 -type structure shows that they can be considered as rock-salt-type layers parallel to the (113) plane of the cubic rock salt structure. Their assemblage through the edges of their octahedra leads to a perfect "TiO" or "TiO" rock salt structure (Fig. 6). Thus the CaTi_2O_4 -type structure (Fig. 3), in which two successive $[\text{Ti}_2\text{O}_4]_\infty$ layers are derived one from the other by a mirror plane, corresponds to a chemical twin of the (113)-oriented rock salt

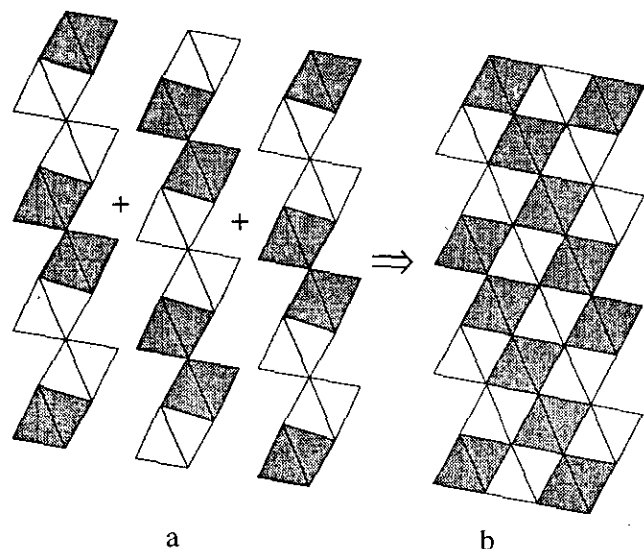


FIG. 6. Assemblage of $[\text{Ti}_2\text{O}_4]_x$ (a) to form the "TiO" rock salt structure (b).

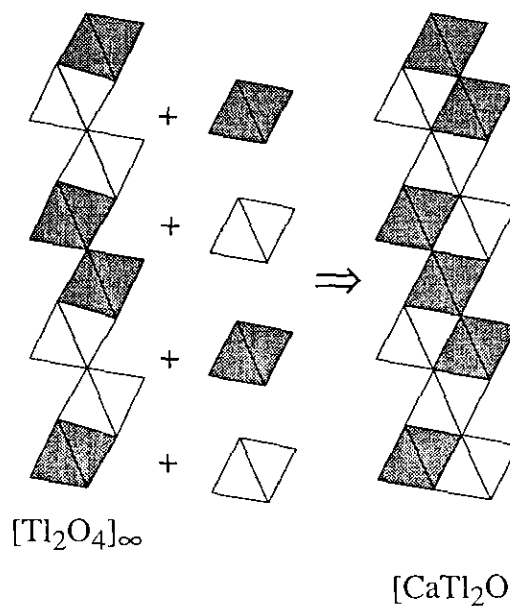


FIG. 7. Assemblage of $[\text{Ti}_2\text{O}_4]_x$ plus rutile chain (a) to form $[\text{CaTi}_2\text{O}_5]_x$ (b).

structure. As already stated above, the $[\text{Ca}_2\text{Ti}_2\text{O}_5]_\infty$ layers of $\text{Ca}_2\text{Ti}_2\text{O}_5$ can be obtained by adding rutile chains to the $[\text{Ti}_2\text{O}_4]_\infty$ layers (Fig. 7); as a result, the $[\text{Ca}_2\text{Ti}_2\text{O}_5]_\infty$ layers still exhibit the rock salt structure and are still parallel to the (113) plane of the cubic rock salt structure. Finally, two successive $[\text{Ca}_2\text{Ti}_2\text{O}_5]_\infty$ layers are chemically twinned (Fig. 5), exactly as for CaTi_2O_4 .

CONCLUDING REMARKS

Two new thallates closely related to the rock-salt- and CaTi_2O_4 -type structures, CaTi_2O_4 and $\text{Ca}_2\text{Ti}_2\text{O}_5$, have been isolated. They correspond to a chemical twinning of the rock salt structure and represent the two first members, $n = 1$ and $n = 2$, of a series of the generic formula $(\text{CaO})_{n-1}\text{CaTi}_2\text{O}_4$ or $\text{Ca}_n\text{Ti}_2\text{O}_{n+3}$. An investigation of the other members of this family is in progress.

REFERENCES

1. Z. Sheng and A. M. Herman, *Nature* **332**, 55 (1988); Z. Sheng and A. M. Herman, *Nature* **332**, 138 (1988).
2. B. Raveau, C. Michel, and H. Hervieu, *Congress of Reactivity of Solids*, Princeton, June 1988; *Solid State Ionics* **32**, 1035 (1989).
3. J. Yu, S. Massidda, and A. J. Freeman, *Physica C* **152**, 273 (1988).
4. R. V. Kasowski, W. Y. Hsu, and F. Herman, *Phys. Rev. B* **38**, 5138 (1988).
5. D. R. Hamann and L. F. Mattheiss, *Phys. Rev. B* **38**, 5138 (1988).
6. D. Jung, M. H. Whangbo, N. Herron, and C. C. Torardi, *Physica C* **160**, 381 (1988).
7. R. V. Schenck and H. K. Müller-Buschbaum, *Z. Anorg. Allg. Chem.* **405**, 197 (1974).
8. R. V. Schenck and H. K. Müller-Buschbaum, *Z. Anorg. Allg. Chem.* **396**, 113 (1973).

9. C. Michel, M. Hervieu, B. Raveau, S. Li, M. Greaney, S. Fine, J. Potenza, and M. Greenblatt, *Mater. Res. Bull.* **26**, 123 (1991); C. Michel, M. Hervieu, V. Caignaert, and B. Raveau, *Acta Crystallogr. Sect. C* **48**, 1747 (1992).
10. J. Rodriguez-Carvajal, in "Satellite Meeting on Powder Diffraction," Abstracts of the XVth Conference on the International Union of Crystallography Toulouse, p. 127, 1990.
11. P. E. Werner, *Z. Kristallogr.* **120**, 375 (1964).
12. E. F. Bertaut and P. Blum, *Acta Crystallogr.* **9**, 121 (1956).
13. P. M. Hill, H. S. Peiser, and J. R. Rait, *Acta Crystallogr.* **9**, 981 (1956).
14. R. D. Shannon, *Acta Crystallogr. Sect. A* **32**, 751 (1976).
15. P. Papamantellos, *Z. Kristallogr.* **126**, 143 (1968).
16. H. H. Otto, R. Boltrusch, and H. J. Brandt, *Physica C* **215**, 205 (1993).
17. C. C. Toraradi, M. A. Subramanian, J. C. Calabrese, J. Gopalakrishnan, E. M. McCarron, K. J. Monisey, T. R. Askew, R. B. Flippen, U. Chowdhry, and A. W. Sleight, *Phys. Rev. B* **38**, 225 (1988).
18. M. A. Subramanian, J. B. Parise, J. C. Calabrese, C. C. Torardi, J. Gopalakrishnan, and A. W. Sleight, *J. Solid State Chem.* **77**, 192 (1988).
19. B. Morosin, D. S. Ginley, P. F. Hlava, M. J. Carr, R. J. Baugman, J. E. Schirber, E. L. Venturini, and J. K. Kwak *Physica C* **152**, 413 (1988).